Ceramics-Silikáty 61 (1), 6-13 (2017)
journal webpage: www.ceramics-silikaty.cz doi: 10.13168/cs.2016.0053

EFFECT OF K_2O AND MgO ON THE FORMATION AND HYDRATION ACTIVITY OF Ba-BEARING CALCIUM SULFOALUMINATE

SHEN WEIBO*, ZHANG YUN*, #GONG CHENCHEN**, XIN JIBAO**

*Institute of soil and water conservation,
Northwest A&F University, Yangling, 712100, China
**Shandong provincial key Laboratory of preparation and measurement of building materials,
University of Jinan, Jinan, 250022, China

#E-mail: 15169028579@163.com, shenwb@ms.iswc.ac.cn

Submitted April 9, 2016; accepted September 17, 2016

Keywords: Ba-bearing calcium sulfoaluminate, MgO, K_2O, Formation, Hydration

Ba-bearing calcium sulfoaluminate ($C_{2.75}B_{1.25}A_3\$$) is characterized by rapid hydration rate and volume stability, as a constituent of the low-CO_2 alternative clinker. In this paper, the effect of K_2O and MgO on the formation and hydration activity of Ba-bearing calcium sulfoaluminate was studied. Results show that according to DSC–TA curves 0.5 - 0.8 wt. % K_2O can reduce the decomposition temperature of $CaCO_3$ about 10-23°C and the decomposition temperature of $C_{2.75}B_{1.25}A_3\$$ about 10 - 16°C. And 4.0 ~ 5.0 wt. % MgO can reduce the decomposition temperature of $CaCO_3$ about 10 - 23°C and the decomposition temperature of $C_{2.75}B_{1.25}A_3\$$ about 10 - 16°C. The effect of MgO on hydration activity of $C_{2.75}B_{1.25}A_3\$$ is a little better than that of K_2O. This may be due to the reason that MgO, especially at the optimum dosage of 3.0 ~ 4.0 wt. %, favors the formation of $C_{2.75}B_{1.25}A_3\$$ mineral with little impurities such as $BaAlO_4$ which is obtained from the analysis of XRD. From the released hydration heat rate and cumulative heat release results it is found that 0.5 - 1.1 wt. % K_2O and 2.0 - 4.0 wt. % MgO promote the hydration of $C_{2.75}B_{1.25}A_3\$$ because of the lattice distortion and defects. Appropriate amount of MgO (2.0 - 4.0 wt. %) and K_2O (0.8 wt. %) can improve the compressive strength and ensure it steady growth with the increase of curing ages. But 1.4 wt. % K_2O and 5.0 wt. % MgO caused $BaSO_4$ and $BaAlO_4$ to extend the hydration of $C_{2.75}B_{1.25}A_3\$$ and reduce the compressive strengths at both early ages and late ages.

INTRODUCTION

Calcium sulfoaluminate ($C_4A_3\$$) is one of the main constituents of a low-CO_2 alternative clinker [1-4], which possesses a rapid hydration rate and is the most abundant constituent of sulfoaluminate cement clinkers in marine engineering and waterproof engineering [5-9]. The substitution of Ba^{2+} for Ca^{2+} to improve the performance of $C_4A_3\$$ has been reported [10-13]. The crystal lattice distortion and defects can be caused by the substitution of barium ions by calcium ions. Cheng Xin et al. [14-17] have synthesized the single crystal of Ba-bearing calcium sulfoaluminate, gained the structural data, and confirmed the relationship of structure and activity of Ba-bearing calcium sulfoaluminate minerals. Besides, it has been found out that Ba-bearing calcium sulfoaluminate ($C_{2.75}B_{1.25}A_3\$$) develops the highest compressive strength in the series of $CaO·xBaO·3Al_2O_3·CaSO_4$ ($C_{3-x}B_xA_3\$$) minerals [18].

Compared with $C_4A_3\$$, $C_{2.75}B_{1.25}A_3\$$ is a more promising mineral, which is characterized by high early strength, good permeability resistance, high corrosion resistance, low alkalinity and so on [19]. The hydrating induction period of $C_{2.75}B_{1.25}A_3\$$ is much shorter than that of C_4A_3S [20]: the hydration of $C_{2.75}B_{1.25}A_3\$$ begins to accelerate at 4 h and most of the hydration heat is released at 4-12 h. By contrast, the hydration of $C_4A_3\$$ mineral begins to accelerate at 23 h and its hydration heat at 42 h is equal to that of $C_{2.75}B_{1.25}A_3\$$ at 12 h. It is thus clear why $C_{2.75}B_{1.25}A_3\$$ mineral has the superior performances in terms of early strength and high strength.

More intention is thus being paid to $C_{2.75}B_{1.25}A_3\$$-C_2S cement. In earlier researches, $C_{2.75}B_{1.25}A_3\$$ was introduced into belite-rich cement to produce belite-$C_{2.75}B_{1.25}A_3\$$ cement, which is a new type of energy-efficient and environmentally friendly cement [21]. It was reported that $C_{2.75}B_{1.25}A_3\$$ enhanced the early age property of this cement compared with belite cement [22-24]. It was known that there exist various minor components in the natural materials (limestone, clay, etc.) for cement production, such as MgO, K_2O and so on. Therefore, it is essential to figure out the influence of MgO and K_2O on the formation and hydration activity of $C_{2.75}B_{1.25}A_3\$$, and currently no such work has been reported.

This study mainly investigates the separate role of K_2O and MgO in the $C_{2.75}B_{1.25}A_3\$$ formation and the hydrating and hardening properties, such as hydration rate, hydration heat release, compressive strength development and microstructures of hydration products. It is hoped that this paper could offer available data for scientific system and further industrial production of belite-barium calcium sulphoaluminate cement.

EXPERIMENTAL

Sample preparation

The samples were synthesized by using analytical chemical regent grades of $CaCO_3$, Al_2O_3, $BaSO_4$ and $BaCO_3$ (99.0 % from Sinopharm Chemical 3sReagent Co., Ltd, China) to eliminate the influences of other impurities as much as possible. K_2O and MgO were separately added into the raw materials of $C_{2.75}B_{1.25}A_3\$$ ($2.75CaO\cdot 1.25BaO\cdot 3Al_2O_3\cdot CaSO_4$), whereas the K_2O and MgO were respectively derived from K_2CO_3 and MgO (99.0 % from Sinopharm Chemical Reagent Co., Ltd, China). Table 1 shows the specific dosages of dopants (percentage in relation to the pure $C_{2.75}B_{1.25}A_3\$$). The pure $C_{2.75}B_{1.25}A_3\$$ without dopants is taken as the blank. The raw materials (finer than 74 μm) were mixed and wetly ground in the planetary mill for 40 minutes to ensure homogenous. Mixtures were then dried and formed 40 mm × 40 mm × 3 mm cubes. After that, the cubes were oven-dried at 105°C for 1-2 h before calcined to 1380°C at a heating rate of 5°C·min^{-1}, held for 2 h and then cooled immediately. The calcined samples were ground to the residue weight of less than 5.0 % for a 74 μm sieve.

Table 1. Dosages of added K_2O and MgO (wt.%).

Dopants	Specific dosages				
K_2O	0	0.5	0.8	1.1	1.4
MgO	0	2.0	3.0	4.0	5.0

The ground samples were mixed with 8.0 wt. % $CaSO_4\cdot 2H_2O$ (99.0 % from Sinopharm Chemical Reagent Co., Ltd, China). Pastes were prepared at a water/cement ratio of 0.35, cast in 20 mm × 20 mm × 20 mm molds and vibrated to remove air bubbles. The molded pastes were kept at 20 ± 2°C and relative humidity exceeding 95.0 % for 12 h, and then removed from the molds. The demolded samples were cured in a water tank at 20 ± 2°C for 1, 3, 7 and 28 days.

Sample testing

Free-CaO tests

The content of free-CaO in cement clinkers was measured according to ethanediol-alcohol method by the fast f-CaO measurement apparatus.

Thermal analysis

Differential scanning calorimetry (DSC) and Thermogravimetric analysis (TGA) test were performed to monitor the reaction process of $C_{2.75}B_{1.25}A_3\$$ mineral formation. The equipment used was a simultaneous thermal analyzer (TGA/DSC) from Mettler Toledo. The dynamic heating ramp varied between 30°C and 1500°C at a heating rate of 10°C·min^{-1} with α-alumina (α-Al_2O_3) as the reference material. Measurements were carried out in alumina crucibles under Argon atmosphere.

X-ray diffraction (XRD)

XRD data were collected on D8 ADVANCE X-ray diffractometer with strictly monochromatic Cu Kα radiation ($\lambda = 0.154$ nm) produced by Bruker in Germany. The overall measurements for samples were carried out in the range of 10° to 60° (2θ) with a step size of 0.02° (2θ), a step time of 4 s per pattern, an accelerating voltage of 40 kV and a current of 40 mA.

Scanning electron microscopy (SEM)

Pieces of hydrated samples at different ages were coated with carbon to provide a conductive surface for SEM imaging. Observation of mineral morphological feature was examined by using a Field Emission Scanning Electron Microscope (GUANTA 250-FEG, USA) with a Link Energy Disperse Spectroscopy (LinkISIS300 type, USA) system. The distribution of elements in minerals was analyzed by Energy Spectrum analysis (EDS).

Hydration heat-evolution test

An isothermal heat-conduction calorimetry (TAM air C80, Thermometric, Sweden) was used to measure the hydration heat evolution of samples mixed with 8.0 wt. % $CaSO_4\cdot 2H_2O$. The water/cement ratio was 0.35 and experimental temperature was 25.0 ± 0.1°C. Samples and water were tempered for several hours before mixing. Then the water was injected into the reaction vessel and the samples were stirred in the calorimeter for several minutes. This procedure allowed monitoring the heat evolution from the beginning when water was added to samples. Data acquisition was performed for about 6 days.

Compressive strength test

Compressive strength tests were carried out according to Chinese standard titled Common Portland Cement (GB 175-2007). The determination of compressive strength was performed after 0.5, 1, 3, 7 and 28 days of hydration, and subsequently the hydration reactions of the pastes were stopped by absolute ethyl alcohol. Each resultant value of compressive strength was an average value calculated from six determinations.

RESULTS AND DISCUSSIONS

The formation of $C_{2.75}B_{1.25}A_3\$$

Thermal analysis

Figure 1 shows the DSC and TG curves of raw mixtures with K_2O. The DSC curves display a number of thermal effects, and TG curves show the associated decarbonation as the main weight loss. Table 2 gives the temperature of peaks labeled in Figure 1. The two small endothermic peaks at about 300°C and 500°C, corresponding to small weight losses, result from the dehydration and dehydroxylation caused by moisture absorption of raw material Al_2O_3 (Wang S. D., 2013). The sharp endothermic peaks between 800°C and 900°C (3# position), with substantial weight losses associated, correspond to the decomposition of $CaCO_3$. It can be seen that the addition of K_2O (0.5 ~ 1.1 wt. %) leads to a lower decomposition temperature of $CaCO_3$, and especially at 0.8 wt. % K_2O, the temperature is decreased by 23°C (Table 2). In contrast, 1.4 wt. % K_2O has little effect on decomposition temperature of $CaCO_3$. This indicates that a certain content of K_2O contributes to the decomposition of $CaCO_3$, which favors the formation of $C_{2.75}B_{1.25}A_3\$$ mineral. Finally, the small peak at about 1400°C in each sample is observed (4# position). This peak is within a large downward trend, due to partial decomposition of $C_{2.75}B_{1.25}A_3\$$. The 5# peak means the massive decomposition of $C_{2.75}B_{1.25}A_3\$$. It is found From Figure 1 and Table 2 that K_2O accelerates the decomposition of $C_{2.75}B_{1.25}A_3\$$, and the decomposition temperature reduces gradually with increasing K_2O dosage. While K_2O reaches the maximum dosage as designed 1.4 wt. %, the temperature is still over 1360°C which is the synthesized temperature of belite-$C_{2.75}B_{1.25}A_3\$$ cement.

Similarly, the thermal analysis of raw mixtures doped with MgO is discussed and the results are shown in Figure 2 and Table 3. Five main endothermic peaks in the samples with MgO are also observed as discussed above. When MgO dosage are respectively 2 wt. % and 3 wt. %, the decomposition of $CaCO_3$ characterized in 800 - 900°C is slightly delayed and the delay is more evident as MgO rises. The decomposition temperature decreases by 10°C at 5.0 wt. % MgO. Meanwhile, the 4# and 5# peaks shift to a lower temperature position with MgO content increasing, which indicates that the presence of MgO plays a positive role in $C_{2.75}B_{1.25}A_3\$$ decomposition. This is in line with the effect of K_2O on its decomposition obtained from Figure 1, but less decline in the decomposition temperature of $C_{2.75}B_{1.25}A_3\$$ appears under the influence of MgO as given in Table 3.

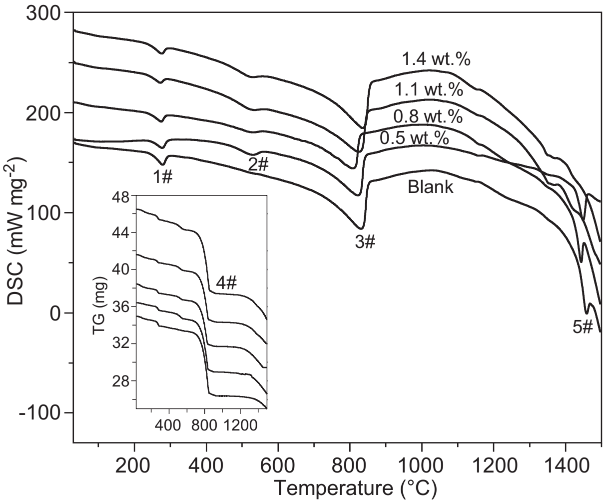

Figure 1. DSC/TG results of raw mixtures doped with K_2O.

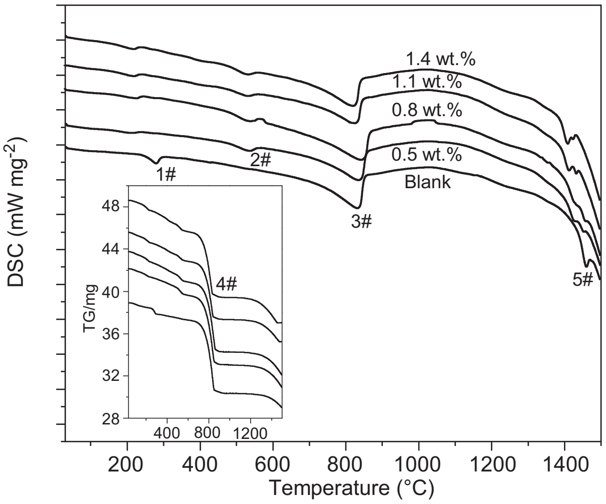

Figure 2. DSC/TG results of raw mixtures doped with MgO.

Table 2. Temperature of the endothermic peaks labeled in Figure 1.

K_2O Dosages (wt. %)	Temperature (°C)				
	1#	2#	3#	4#	5#
0.0	279.3	–	831.3	1373.2	1458.5
0.5	277.4	529.2	822.8	1324.6	1448.4
0.8	275.6	523.9	808.6	1308.2	1442.9
1.1	273.0	527.2	825.0	1281.9	1377.1
1.4	276.8	523.9	835.6	1274.5	1360.6

Table 3. Temperature of the endothermic peaks labeled in Figure 2.

MgO Dosages (wt. %)	Temperature (°C)				
	1#	2#	3#	4#	5#
0.0	279.3	-	831.3	1373.2	1458.5
2.0	218.1	538.8	835.4	1325.9	1430.1
3.0	227.5	539.3	842.2	1302.3	1423.6
4.0	219.5	532.6	825.5	1288.4	1417.1
5.0	219.9	526.3	819.4	1274.5	1401.2

XRD analysis

XRD patterns of $C_{2.75}B_{1.25}A_3\$$ doped with K_2O are shown in Figure 3. It can be seen that compared to the blank though the characteristic diffraction peaks (d = 0.3787 nm, d = 0.2681 nm) of $C_{2.75}B_{1.25}A_3\$$ at about 23.5°and 33.4°(2θ) vary little with doping K_2O, those (2θ = 41.2°) are more evident and sharper. It is indicated that added K_2O promotes the formation of $C_{2.75}B_{1.25}A_3\$$ mineral. The peaks (2θ = 41.2°) of $C_{2.75}B_{1.25}A_3\$$ with 0.5 wt. % and 0.8 wt. % K_2O become higher than those with 1.1 wt. % and 1.4 wt. % K_2O. It means that too much K_2O limits the formation of $C_{2.75}B_{1.25}A_3\$$. Besides $C_{2.75}B_{1.25}A_3\$$, small amounts of $BaSO_4$ and $BaAlO_4$ as the impurities are present in the samples.

It is noted that the peak intensity (2θ = 19.7°) of $BaSO_4$ remarkably decreases with K_2O dosage of 0.5 wt. % and 0.8 wt. % while it heightens as K_2O content rises. Similarly, the $BaAlO_4$ peak at about 28.4° (2θ) shows the same trend. These variations suggest that synthesized $C_{2.75}B_{1.25}A_3\$$ mineral has fewer impurities when K_2O dosages are 0.5 wt. % and 0.8 wt. %. Thus, it can be conclude that 0.5 ~ 0.8 wt. % K_2O is favorable for the formation of $C_{2.75}B_{1.25}A_3\$$ mineral.

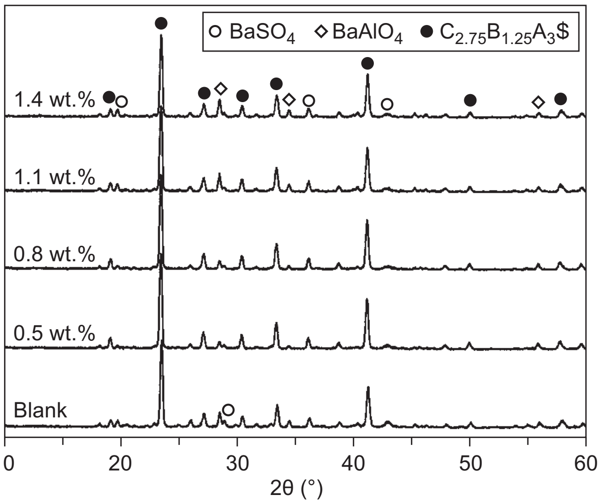

Figure 3. XRD patterns of $C_{2.75}B_{1.25}A_3\$$ doped with K_2O.

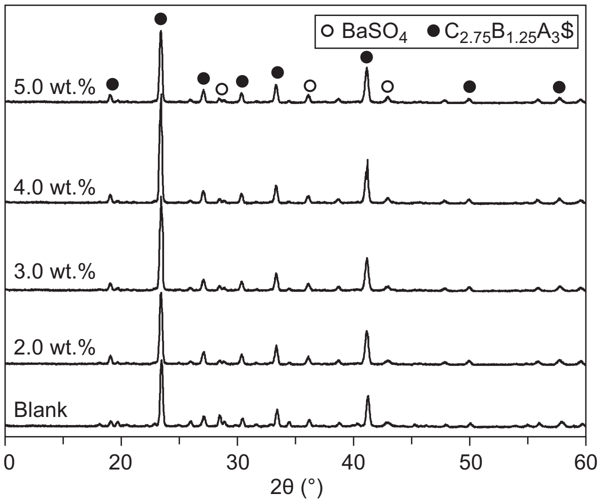

Figure 4. XRD patterns of $C_{2.75}B_{1.25}A_3\$$ doped with MgO.

Figure 4 is the XRD patterns of $C_{2.75}B_{1.25}A_3\$$ doped with MgO. Different from the sample with K_2O, no $BaAlO_4$ peaks appear in the samples doped with MgO. Moreover, the intensities of $BaSO_4$ peaks (d = 0.3092 nm, d = 0.2488 nm, d = 0.2100 nm) change little with MgO dosage increasing. This indicates that MgO makes significant sense to the synthesis of pure $C_{2.75}B_{1.25}A_3\$$ mineral. Besides, it is clearly observed in Figure 4 that characteristic peaks of $C_{2.75}B_{1.25}A_3\$$ (d = 0.3787 nm, d = 0.2681 nm) obviously strengthen when the MgO dosage is 4.0 wt. %, and the intensity of $C_{2.75}B_{1.25}A_3\$$ peaks increases to the maximum. However, the peak at about 23.5° is obviously weakened when MgO dosage reaches to 5.0 wt. %. This illustrates that MgO promotes the formation of $C_{2.75}B_{1.25}A_3\$$ mineral at the dosage of 3.0 ~ 4.0 wt. %. Additionally, it can be seen that the characteristic diffraction peak of $C_{2.75}B_{1.25}A_3\$$ mineral (2θ = 23.5°) shifts to a lower diffraction angel position with increasing MgO content. This may be due that Mg^{2+} partially substitutes Ca^{2+} or Ba^{2+} in the same main group elements in the periodic Table of chemical elements and this results in a rise in the interlunar spacing.

Morphology and mineralogy analysis

Monocrystal $C_{2.75}B_{1.25}A_3\$$ has a complete crystal shape belonging to rhombic dodecahedron (Cheng X., 2013). Whereas, $C_{2.75}B_{1.25}A_3\$$ mineral is usually not regular rhombic dodecahedron, but close to the dodecahedron or shape of sphere (Wang S. D., 2013; Wang C. P., 2005). Regarding the results of Figure 3 and Figure 4, only SEM and EDS pictures of samples optimized by appropriate K_2O and MgO are illustrated in Figure 5. As shown from Figure 5a, the pure $C_{2.75}B_{1.25}A_3\$$ mineral in our study is nearly of small size of 0.5 ~ 2 µm with the spherical shape, and parts are wrapped in each other with unclear grain boundary. However, from Figure 5b, it is found that there is a morphology of sphere and polyhedron, and grains grow well with clear grain boundaries. Moreover, K_2O favors the formation of $C_{2.75}B_{1.25}A_3\$$ crystals with big size. In the sample with 0.8 wt. %, the particles are uneven distributed with the size ranging from 0.3µm to 3µm. Under the influence of MgO, the $C_{2.75}B_{1.25}A_3\$$ mineral generally occurs as regular smooth and round appearance but the boundaries between grains are not very clear (Figure 5c). Furthermore, small particles and homogeneous distribution are observed, compared with the blank and the samples with K_2O. At 4 wt. % MgO, particle size is in the range of 0.3 ~ 1 µm, which may further enhance the hydration of $C_{2.75}B_{1.25}A_3\$$ mineral. In general, $C_{2.75}B_{1.25}A_3\$$ mineral grains form well with clear grain boundaries when dopants are added.

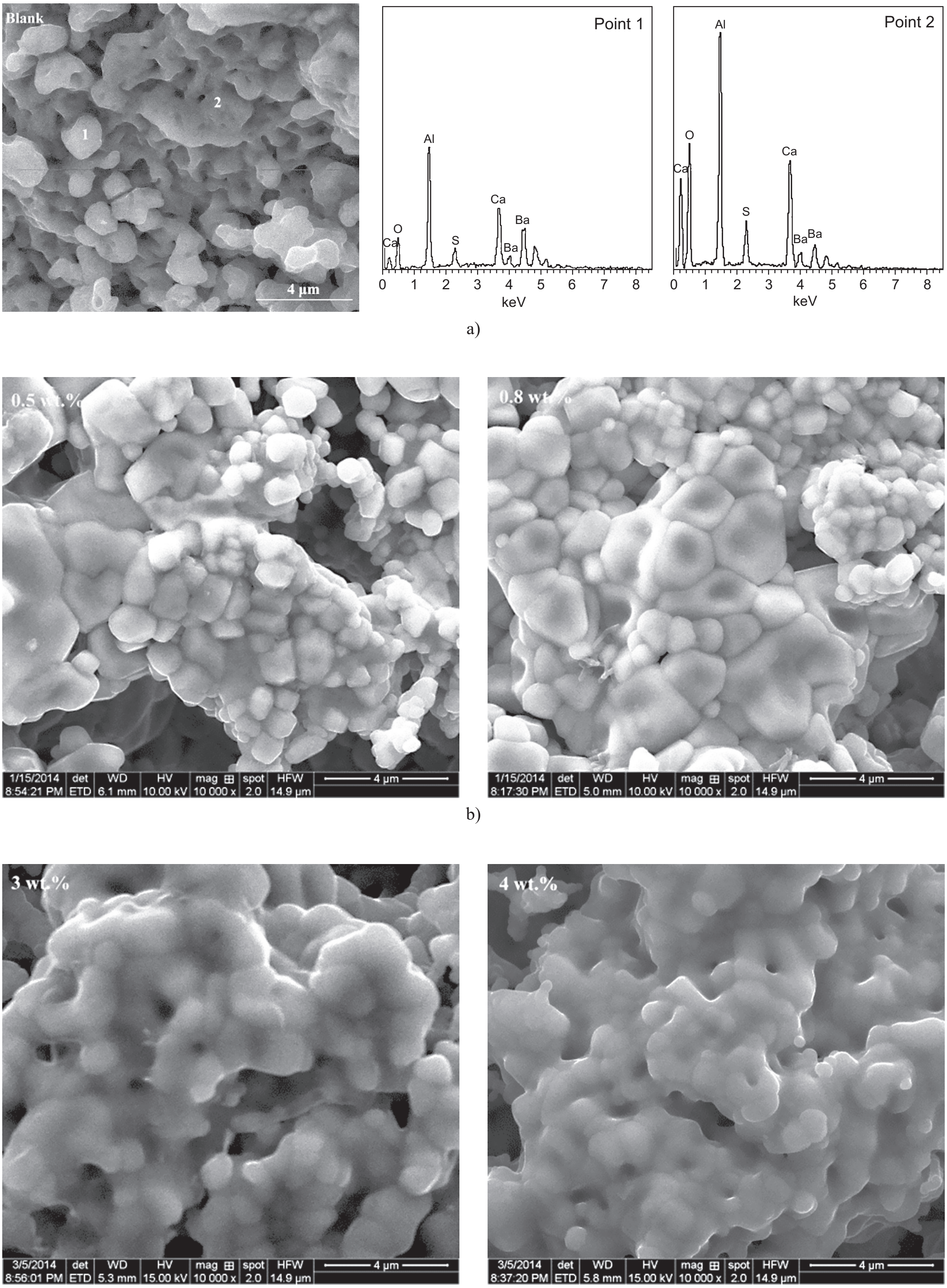

a)

b)

c)

Figure 5. SEM-EDS images of various samples. (a) the blank, (b) sample with K_2O, (c)sample with MgO.

The hydration activity and mechanical property

Hydration heat analysis

It has been reported that the hydration of $C_{2.75}B_{1.25}A_3\$$ includes five stages: initial hydration period, induction period, acceleration period, deceleration period and stabilization period (Chang J., 2002). To reflect the effect of K_2O and MgO on the early-age hydration activity of $C_{2.75}B_{1.25}A_3\$$ in detail, the hydration heat liberations of studied samples during 24 hours are measured as shown in Figure 6 and Figure 7, respectively.

Figure 6 respectively displays released hydration heat rate and cumulative heat release of samples doped with K_2O. Obviously, added K_2O with various dosages has different influences on the hydration reaction. Rather intense heat liberation within few minutes is due to the initial rapid hydration of $C_{2.75}B_{1.25}A_3\$$ in the pre-induction period. It can be seen that the first signal in sample with 1.4 wt. % K_2O occurs 10 minutes later in the initial hydration than that of other samples (Figure 6a). Soon thereafter, the overall rate of hydration is slowed down in the induction period. The end time of the induction period has an important effect on the hydration. As shown from Figure 6a, 1.4 wt. % K_2O has an adverse effect on hydration reaction of $C_{2.75}B_{1.25}A_3\$$, which retards the induction period nearly 6 hours compared with the blank. This delay is also observed from the accumulated hydration heats (Figure 6b). It was explained that 1.4 wt. % K_2O caused the formation of $BaSO_4$ and $BaAlO_4$ in Figure 3which had no or little hydrating activity. However, the hydration process significantly accelerates with less K_2O added. At 0.8 wt. % MgO, the second big broad signal appears firstly, and then in one hour there also exists the singal in the sample with 0.5 wt. % K_2O. The accumulated hydration heats with 0.5 wt. % and 0.8 wt. % are 510 $J \cdot g^{-1}$ and 498 $J \cdot g^{-1}$, respectively. 0.5 - 1.1 wt. % K_2O could cause lattice distortion and defects during the formation of $C_{2.75}B_{1.25}A_3\$$, which was favorable to hydrating activity of $C_{2.75}B_{1.25}A_3\$$. The phenomena indicate that high amount of K_2O (1.4 wt. %) has noticeable retarding effects, while appropriate amount of K_2O (< 1.1 wt. %) plays a significant role in the hydration process.

The hydration heat flow and cumulative heat release of samples doped with MgO are illustrated in Figure 7. It can be seen that there are few differences among the studied samples in the initial hydration, which all happen in 15 minutes (Figure 7a). However, for the following stage there exists a big difference between the samples with and the blank. It is clear that MgO remarkably shortens the induction period. The acceleration period of the sample with 5.0 wt. % MgO appears over 6 hours earlier than that of the blank. The induction period of the sample with 4.0 wt. % MgO is comparable with that of the sample with 3.0 wt.% MgO while the hydration rate of 4.0 wt. % MgO sample is the largest as high as 0.072 $W \cdot g^{-1}$. Meanwhile, the stabilization period of samples with MgO nearly arrives after 8 h. However, for the blank it occurs after 14 h. This means that MgO distinctly enhances the hydration activity of $C_{2.75}B_{1.25}A_3\$$. From Figure 6b. It can be discovered that how long the total heat release approaches corresponds with the rate of heat release. On the other hand, it can be seen that MgO helps the acceleration period of hydration arrive within 4 hours except for the sample with 2.0 wt. %. In contrast, the acceleration periods of samples with 0.5 ~ 1.1 wt. % K_2O appear within 7 h, which are 3 hours later than those of samples with 3.0 ~ 5.0 wt. % MgO. Furthermore, the maximum hydration rate of 0.5 wt. % K_2O-doped sample is about 0.045 $W \cdot g^{-1}$, which is smaller than that of 4.0 wt. %-doped MgO of 0.072 $W \cdot g^{-1}$. It is indicated that the effect of MgO on hydration activity of $C_{2.75}B_{1.25}A_3\$$ is a little better than that of K_2O. This may be due to the reason that MgO, especially at the optimum dosage of 3.0 ~ 4.0 wt. %, favors the formation of $C_{2.75}B_{1.25}A_3\$$ mineral with little impurities which is obtained from the analysis of Figure 3 and Figure 4. Besides, the results are also supported by the results of Figure 5.

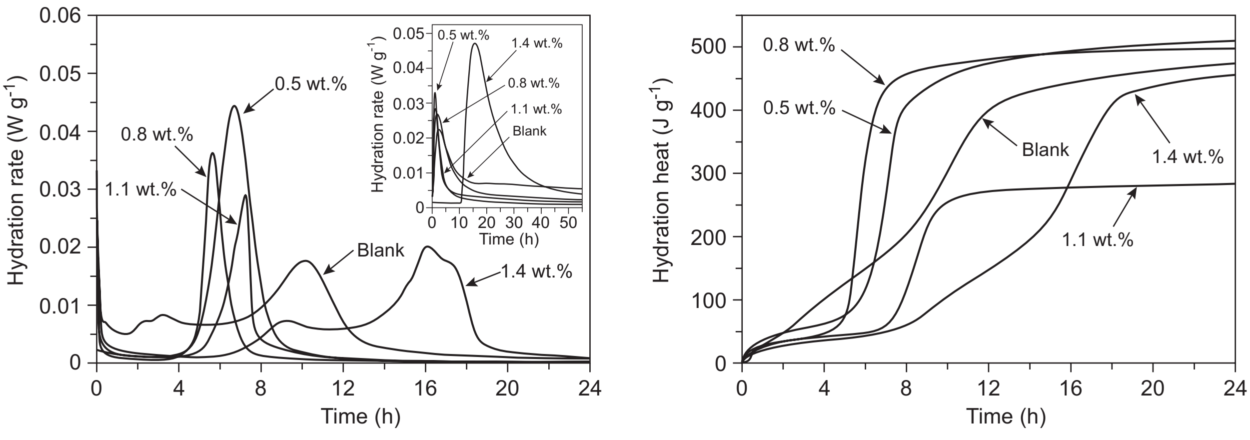

a) b)

Figure 6. Calorimetric heat flows and heat curves for samples doped with K_2O (w/c = 0.35); a) rate of heat liberation, b) total heat evolved.

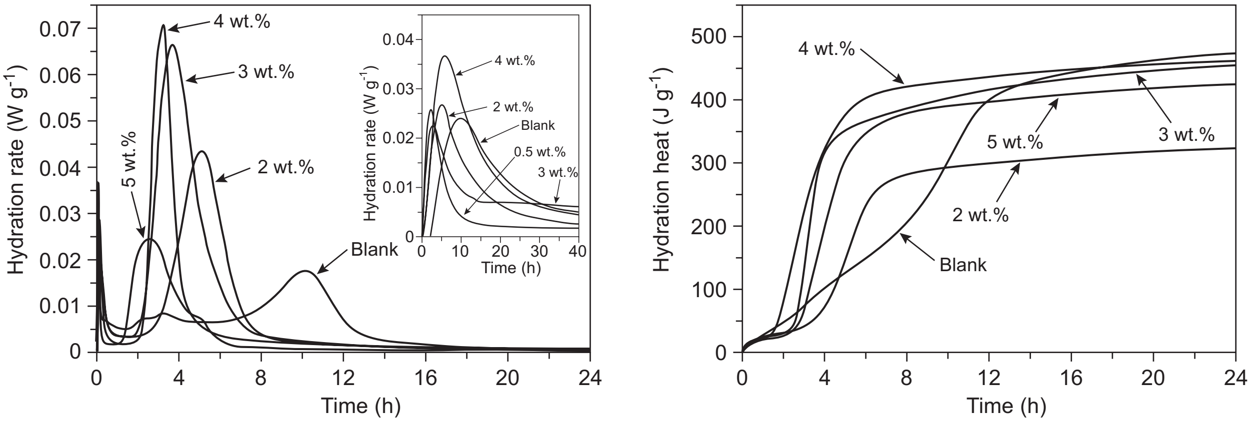

a) b)

Figure 7. Calorimetric heat flows and heat curves for samples doped with MgO (w/c = 0.35); a) the rate of heat liberation, b) total heat evolved.

Compressive strength

Pictorial diagrams of the compressive strengths of cementitiou materials are provided in Figure 8, and Table 4 gives the strength increase rates of others doped with K_2O or MgO. Figure 8 shows that the compressive strengths of all cementitiou materials increase with increasing curing time. It is apparent that doped K_2O and MgO separately have different influences on the compressive strengths. Compared with the blank, 0.8 wt. % K_2O is helpful to the compressive strengths, especially at the early curing time. The compressive strengths of cementitious material with 0.8 wt. % K_2O at 0.5 d and 1 d are 38 % and 33 % higher than the blank, respectively. But the compressive strengths of cementitious material with 1.4 wt. % K_2O are less than the blank at the same curing time. Appropriate amount of K_2O improves the compressive strength while high content of K_2O (1.4 wt. %) lead to an adverse effect. All results discussed here are in accordance with the previous results of Figure 6.

Compared with the blank, it is helpful for the compressive strengths to add 2.0 wt. % MgO and 4.0 wt. % MgO, especially at the early curing time. And with the increasing MgO addition, the compressive strengths increase. The compressive strengths of cementitious material with 4.0 wt. % MgO at 0.5 d ,1 d and 28 d are 47 % , 56 % and 13 % higher than the blank, respectively. Appropriate amount of MgO (2.0 - 4.0 wt. %) improves the compressive strength. All results discussed here are in accordance with the previous results of Figure 7.

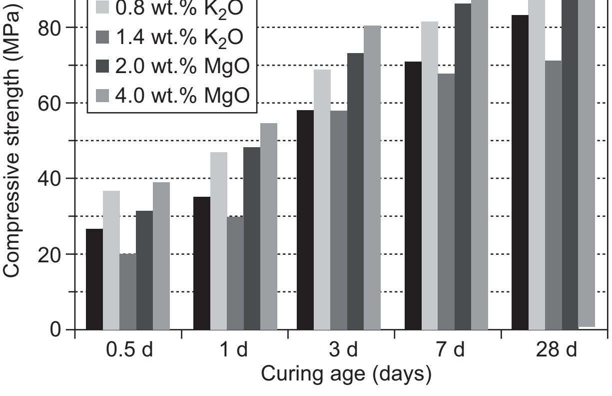

Figure 8. Compressive strengths of studied pastes.

Table 4. Strength increasing rate of samples with additions relative to the blank sample/%.

Sample Label	Strength improvement rate				
	0.5 d	1 d	3 d	7 d	28 d
0.8 wt. % K_2O	38	33	18	15	5
1.4 wt. % K_2O	-25	-42	-1	-5	-14
2.0 wt. % MgO	18	37	26	22	8
4.0 wt. % MgO	47	56	39	27	13

CONCLUSIONS

In this paper, from the basis of multiple perspectives, we studied the influence of K_2O and MgO on the formation and hydration activity of $C_{2.75}B_{1.25}A_3\$$. Major conclusions can be drawn as follows:

- According to DSC-TA curves 0.5 - 0.8 wt. % K_2O can reduce the decomposition temperature of $CaCO_3$ about 10 - 23°C and the decomposition temperature of $C_{2.75}B_{1.25}A_3\$$ about 10 - 16 °C. And 4.0 ~ 5.0 wt. % MgO can reduce the decomposition temperature of $CaCO_3$ about 10 - 23°C and the decomposition temperature of $C_{2.75}B_{1.25}A_3\$$ about 10 - 16°C. So 0.5 ~ 0.8 wt. % K_2O and 4.0 ~ 5.0 wt. % MgO can respectively promote the decomposition of $CaCO_3$ and lower the decomposition temperature of $C_{2.75}B_{1.25}A_3\$$ mineral.

- 0.5 - 0 .8 wt. % K_2O is favorable for the formation of $C_{2.75}B_{1.25}A_3\$$ mineral. Too much K_2O limits the formation of $C_{2.75}B_{1.25}A_3\$$. When K_2O content reaches up to 1.4 wt. %, small amounts of $BaSO_4$ and $BaAlO_4$ as the impurities are present. At the same time 3.0 ~ 4.0 wt. % MgO promotes the formation of $C_{2.75}B_{1.25}A_3\$$. mineral Additionally, the characteristic diffraction peak ($2\theta = 23.5°$) of $C_{2.75}B_{1.25}A_3\$$ mineral shifts to a lower diffraction angel position with increasing MgO content due to the partial replacement of Mg^{2+} to Ca^{2+} or Ba^{2+}.
- From the released hydration heat rate and cumulative heat release results it is found that 0.5 - 1.1 wt. % K_2O and 2.0 - 4.0 wt. % MgO promote the hydration of $C_{2.75}B_{1.25}A_3\$$ because of the lattice distortion and defects. But 1.4 wt. % K_2O and 5.0 wt. % MgO caused $BaSO_4$ and $BaAlO_4$ to extend the hydration of $C_{2.75}B_{1.25}A_3\$$.
- Appropriate amount of MgO (2.0-4.0 wt. %) and K_2O (0.8 wt. %) can improve the compressive strength and ensure it steady growth with the increase of curing ages. But 1.4 wt. % K_2O can reduce the compressive strengths at both early ages and late ages.

REFERENCES

1. Gartner E. (2004): Industrially interesting approaches to “low-CO_2” cements. *Cement and Concrete Research*, *34*(9), 1489-1498. doi:10.1016/j.cemconres.2004.01.021.
2. Odler I., Zhang H. (1996): Investigations on high SO_3 Portland clinkers and cements I: Clinker synthesis and cement preparation. *Cement and Concrete Research*, 26, 1307-1313. doi:10.1016/0008-8846(96)00128-7.
3. Zhang H., Odler I. (1996): Investigations on high SO_3 portland clinkers and cements II. Properties of cements. Cement and Concrete Research, 26(9), 1315-1324. doi:10.1016/0008-8846(96)00129-9.
4. Ma B., Ma M., Shen X., Li X., Wu X. (2014): Compatibility between a polycarboxylate superplasticizer and the belite-rich sulfoaluminate cement: Setting time and the hydration properties. Construction and Building Materials, 51, 47-54. doi:10.1016/j.conbuildmat.2013.10.028
5. Fukuda N. (1961): Investigation of compound compositions of sulpho-aluminous cement. Journal of the Ceramic Society of Japan, 69, 187-191.
6. Majling J., Sahu S., Vlna M., Roy D. M. (1993): Relationship between raw mixture and mineralogical composition of sulphoaluminate belite clinkers in the system CaO SiO_2 Al_2O_3 Fe_2O_3 SO_3. Cement and Concrete Research, 23(6), 1351-1356. doi:10.1016/0008-8846(93)90072-H
7. Sahu S., Majling, J. (1994): Preparation of sulphoaluminate belite cement from fly ash. Cement and Concrete Research, 24(6), 1065-1072. doi:10.1016/0008-8846(94)90030-2
8. Sahu S., Majling J. (1993): Phase compatibility in the system CaO SiO_2 Al_2O_3 Fe_2O_3 SO_3 referred to sulphoaluminate belite cement clinker. Cement and Concrete Research, 23(6), 1331-1339. doi:10.1016/0008-8846(93)90070-P
9. Ma B., Shen X. Mao Y., Shen X (2013): Synthesis and cha-racterization of high belite sulfoaluminate cement through rich alumina fly ash and desulfurization gypsum. *Ceramics- Silikáty*, 57, 7-13.
10. Teoreanu I., Muntean M., Dragnea I. (1986): Type $3(CaO·Al_2O_3)·Mx(SO_4)y$ compounds and compatibility re-lations in $CaO\text{-}CaO·Al_2O_3\text{-}Mx(SO_4)y$ systems. *Il Cemento*, *83*, 39-46.
11. Yan P. (1993). Hydration of Sr-and Ba-bearing sulphoaluminates in the presence of sulphates. *Advances in Cement Research*, *5*(18), 65-69. doi:10.1680/adcr.1993.5.18.65
12. Cheng X., Yu J., Liu F., Yue Y., Chang J. (1997): Predictions on the formation and bond performance of some ettringites by a quantum chemistry method. Cement and Concrete Research, *27*(7), 1085-1092. doi:10.1016/S0008-8846(97)00091-4.
13. Chang J. (1998). Study on new type Ba-bearing cement. *Mater's Thesis, Wuhan University of Technology, Wuhan, China*.
14. Cheng X., Chang J., Lu L., Liu F., Teng B. (2000): Study of Ba-bearing calcium sulphoaluminate minerals and cement. Cement and Concrete Research, *30*,77-81. doi:10.1016/S0008-8846(99)00204-5
15. Chang J., Cheng X., Liu F., Lu L., Teng B. (2001): Influence of fluorite on the Ba-bearing sulphoaluminate cement. *Cement and Concrete Research*, *31*(2), 213-216. doi:10.1016/S0008-8846(00)00450-6
16. Chang J., Cheng X., Lu L. (2002). Research on using barium industry residue to fire Portland cement, in: *5th Inter-national Symposium on Cement and Concrete*. Shanghai, pp. 786-790.
17. Cheng X. (2013). Barium (strontium) calcium sulphoaluminate cements. 1st ed. Science press, pp. 4-38.
18. Cheng X. Chang J., Lu L. Liu F., Teng B. (2004): Study on the hydration of Ba-bearing calcium sulphoaluminate in the presence of gypsum. *Cement and Concrete Research*, *34*(11), 2009-2013. doi:10.1016/j.cemconres.2004.02.021.
19. Zhang J., Gong C., Wang S., Lu L., Cheng X. (2015): Effect of strontium oxide on the formation mechanism of dicalcium silicate with barium oxide and sulfur trioxide. *Advances in Cement Research*, *27*(7), 381-387. doi:10.1680/adcr.14.00021.
20. Wang S., Huang Y., Gong C., Lu L., Cheng X. (2014): Formation mechanism of barium calcium sulfoaluminate mineral. *Advances in Cement Research*, *26*(3), 169-176. doi:10.1680/adcr.13.00016.
21. Lu L., Zhang W., Ye Z. (2007). Belite-barium calcium sulphoaluminate cement. Chinese Patent, 2007, ZL 200610045503.6.
22. Zhang W., Lu L., Chang J. (2007): Preparation and mechanical performance of Belite-calcium barium sulphoaluminate cement (in Chinese). J*ournal of the Chinese Ceramic Society*, *26*, 345-400.
23. Zhang W., Lu L., Cui Y., Chang J., Cheng X. (2007): Microstructure and performances of belite-calcium barium sulphoaluminate cement. *Journal of the Chinese Ceramic Society*, *35*(4), 467-471.
24. Lu L., Zhang W., Xuan H. (2008): Calcination and condition of belite-calcium barium sulphoaluminate cement and its properties (in Chinese). *Journal of the Chinese Ceramic Society*, *36*(S1), 166-169.